Chemistry
A European
Journal

Chemistry Europe
European Chemical Societies Publishing

Accepted Article

Title: An Imidazolium-based Lipid Analogue as Gene Transfer Agent

Authors: Tiffany O. Paulisch, Steffen Bornemann, Marius Herzog, Sergej Kudruk, Lena Roling, Anna Livia Linard Matos, Hans-Joachim Galla, Volker Gerke, Roland Winter, and Frank Glorius

To be cited as: *Chem. Eur. J.* 10.1002/chem.202003466

Link to VoR: https://doi.org/10.1002/chem.202003466

WILEY-VCH

10.1002/chem.202003466

WILEY-VCH

RESEARCH ARTICLE

An Imidazolium-based Lipid Analogue as Gene Transfer Agent

Tiffany O. Paulisch,[a]+ Steffen Bornemann,[b]+ Marius Herzog,[b]+ Sergej Kudruk,[c]+ Lena Roling,[a] Anna Livia Linard Matos,[c] Hans-Joachim Galla,[d] Volker Gerke,*[c] Roland Winter,*[b] Frank Glorius*[a]

[a] T. O. Paulisch, Dr. L. Roling, Prof. Dr. F. Glorius
Institute of Organic Chemistry, University of Münster, Corrensstraße 40, D-48149 Münster, Germany
glorius@uni-muenster.de
[b] Dr. S. Bornemann, M. Herzog, Prof. Dr. R. Winter
Physical Chemistry I - Biophysical Chemistry, TU Dortmund University, D-44221 Dortmund, Germany
roland.winter@tu-dortmund.de
[c] S. Kudruk, A. L. Linard Matos, Prof. Dr. V. Gerke
Institute of Medical Biochemistry, University of Münster, D-48149 Münster, Germany
gerke@uni-muenster.de
[d] Prof. Dr. H.-J. Galla
Institute of Biochemistry, University of Münster, D-48149 Münster, Germany
+ These authors contributed equally to this work.

Supporting information for this article is given via a link at the end of the document.

Abstract: A novel, dicationic imidazolium salt is described and investigated towards its application for gene transfer. The polar head group and the long alkyl chains in the backbone contribute to a lipid-like behavior, while an alkyl ammonium group provides the ability for crucial electrostatic interaction for the transfection process. Detailed biophysical studies regarding its impact on biological membrane models and the propensity of vesicle fusion are presented. Fluorescence spectroscopy, atomic force microscopy and confocal fluorescence microscopy show that the imidazolium salt leads to negligible changes in lipid packing, while displaying distinct vesicle fusion properties. Cell culture experiments reveal that mixed liposomes containing the novel imidazolium salt can serve as plasmid DNA delivery vehicles. In contrast, a structurally similar imidazolium salt without a second positive charge showed no ability to support DNA transfection into cultured cells. Thus, we introduce a novel and variable structural motif for cationic lipids, expanding the field of lipofection agents.

Introduction

In the context of gene therapy, one major challenge is the controlled insertion of foreign nucleic acids into a target cell, enabling the expression of these genes in the target. This process called gene transfection has been a major focus of pharmaceutical research within recent decades and can be realized by different physical, biological and chemical means.[1] Especially the transport *via* viral vectors and lipoplexes was applied in gene therapy.[2] Transfection through viral vectors has shown high transfection efficiency *in vivo*, but the risk of an immune response presents a major drawback.[3] An alternative approach for gene transfection, namely lipofection, is based on the transport of nucleic acids enclosed in liposomes or covered in sheets of cationic lipid membranes. Such cationic lipids complex the negatively charged cargo due to their positively charged head group, concealing the negative charge of the genetic material, and therefore enabling the passage through the anionic lipid bilayer (see Scheme 1).[4] In comparison to viral vectors, the preparation of lipoplexes is rather simple, since mixing of the cationic lipids with the negatively charged cargo leads to the desired nucleic acid - lipid complex.[5] It is thought that the cationic lipoplex is attracted by the anionic biological target membrane and enables the delivery of the negatively charged genetic material into the cytosol by direct fusion or endocytosis – presumably *via* induction of transient and local non-lamellar phases in the lipoplex membrane.[6]
Despite its currently low *in vivo* efficiency, non-viral gene transfer represents a promising alterative since the methodology is expected to be immunologically inert and it is convenient to prepare the aforementioned lipoplexes. To address current challenges such as *in vivo* transfection efficiencies, accessible synthesis of the cationic lipids and cellular specifications, a series of different cationic lipids and polymers have been introduced.[7] In this regard, we hypothesized that, owing to their inherent positive charge, imidazolium salts could serve as potent transfection agents.

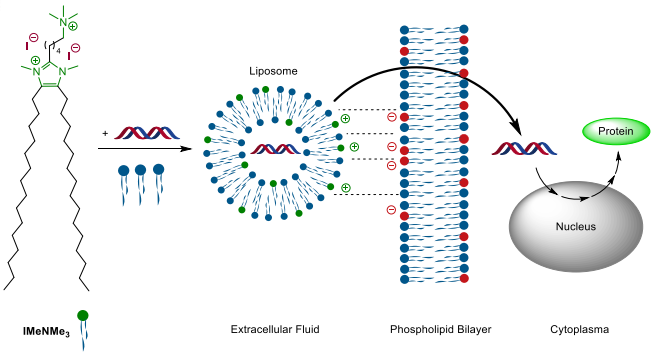

Scheme 1. Design of a dicationic imidazolium-based lipid **IMeNMe$_3$** for application as a gene transfer reagent. Blue – neutral lipids (i.e. DPPC, DOPE, DOPC), Red – negatively charged lipids (i.e. DOPG, DPPG), Green – imidazolium-based lipid analogue.[8]

Within the last years, imidazolium salts have gained considerable attention across diverse fields of chemistry, biology and material sciences. Their function as precursors for N-heterocyclic carbenes has made them essential for both transition-metal and organocatalysis.[9] Moreover, their facile synthesis allows for the

10.1002/chem.202003466

design of tailor-made molecules – installing up to five different substituents on the five-membered heterocycle.[10]

This structural diversity has led to the development of important applications in the field of ionic liquids and also in biological contexts, where imidazolium salts can serve as artificial anion transporters, as medication for cancer treatment or as antimicrobial and antifungal drugs.[11,12,13] Furthermore, recent studies showed remarkable membrane activities of imidazolium salts,[14] and demonstrated pronounced detergent-like properties depending on their alkyl chain length and cationic headgroup structure.[15,12] In this context, we could show in previous studies, that 1,3-dimethyl-4,5-dipentadecylimidazolium (**IMeH**) can be considered a phospholipid bioisostere. The long alkyl chains in positions C4 and C5 provide the non-polar tails, while the imidazolium head serves as the hydrophilic counterpart. The inherent positively charged heterocycle is proposed to interact electrostatically with phosphate groups of the neighboring phospholipids, while the alkyl chains with a length of C_{15} interact with the fatty acids of the phospholipids, cooperatively facilitating membrane integration of the molecule.[12]

Based on this lipid analogue behavior, we propose a novel, dicationic imidazolium salt (**IMeNMe$_3$**) as the parent compound for a new class of lipofection agents (see Scheme 1). We envisioned that, in analogy to our previous work, instead of the common glycerol linker of many cationic lipids, a dimethyl imidazolium scaffold could serve directly as the hydrophilic head group. For supporting membrane integration the long alkyl chains are installed in the backbone. To enable lipofection, a quaternary ammonium salt is installed as a second positive charge at the head group. The attachment at the C2 position of the imidazolium core leads to a highly directional substitution pattern, which should, once incorporated into a membrane, lead to an exposure of the positive charge on the membrane surface. As such, favorable electrostatic interactions with nucleic acids and a negatively charged cell surface should induce a high degree of transfection.

As depicted in Scheme 2A, the synthetic route towards these imidazolium salts allows for facile diversification and could give access to easily modifiable tailor-made transfection reagents. While the backbone can be adjusted in its lipophilic character, the substitution pattern at the heteroatoms determines the integration into the membrane. Most importantly the directional anchor at the C2 position can be adjusted in length and exposition of the positive charge (see Scheme 2B), providing the framework for a series of easily accessible, novel and unique transfection reagents, based on an imidazolium-based phospholipid analogue.

Results and Discussion

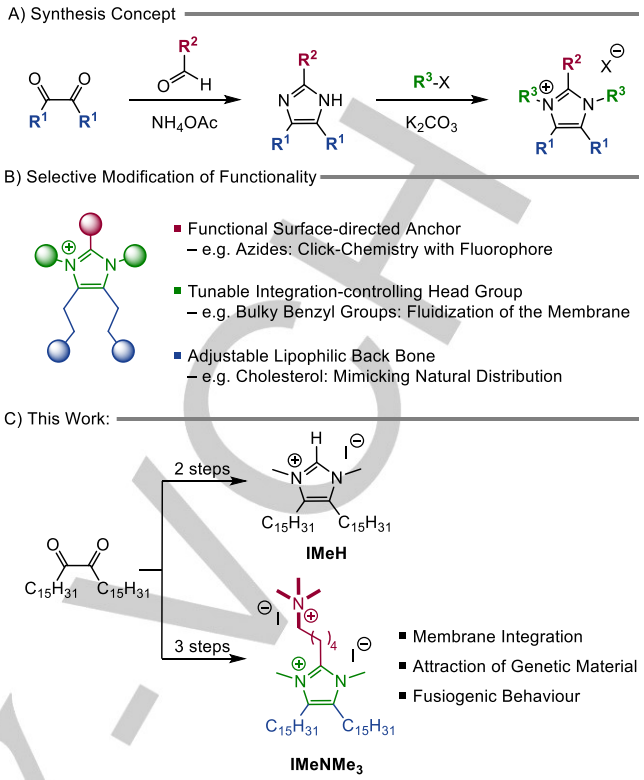

Scheme 2. A) Synthesis concept: Preparation of imidazolium-based phospholipid analogues with different head groups. B) Selective modification of functionality: Installing different substituents effects the properties of the molecule. C) This work: Synthesis of **IMeNMe$_3$** – i) *tert*-butyl (6-oxohexyl)carbamate, NH_4OAc, EtOH, HOAc, 110 °C, 18 h ii) TFA, CH_2Cl_2, rt, 18 h, iii) MeI, K_2CO_3, THF, rt, 18 h. **IMeH** – i) paraformaldehyde, NH_4OAc, EtOH, HOAc, 110 °C, 4 h ii) MeI, K_2CO_3, MeCN, 90 °C, 18 h.

For this study, both the established 1,3-dimethyl-4,5-dipentadecyl-imidazolium iodide (**IMeH**)[12] and the novel 1,3-dimethyl-4,5-dipentadecyl-2-(5-(trimethylammonio)pentyl)imidazolium iodide (**IMeNMe$_3$**) salts were synthesized from the corresponding symmetrical diketone. Condensation with ammonia and a respective aldehyde, followed by exhaustive methylation, allows for the formation of structural C2-diversified phospholipid analogues in a divergent fashion. As such, condensation with an N-protected aminoaldehyde, followed by deprotection and methylation, led to the desired compound **IMeNMe$_3$** (Scheme 2; see SI for more details). Following this divergent synthesis route, tailor-made derivatives are easily accessible.

To prove our hypothesized molecular design and substantiate the proposed activity of **IMeNMe$_3$** as a gene transfectant a series of biophysical investigations were conducted. In the following experiments, model biomembranes of different complexities were used: 1-component: DPPC; 3-component: DPPC:DOPC:cholesterol (2:1:1) or DPPC:DOPE:cholesterol (2:1:1) and 5-component: DPPC:DPPG:DOPC:DOPG:cholesterol (45:5:20:5:25).[8] The latter system served as a refined model of a biological plasma membrane, since it contained anionic lipids in the order of 10 mol%. In all of these membranes, **IMeNMe$_3$** was treated as a partial DPPC replacement.

10.1002/chem.202003466

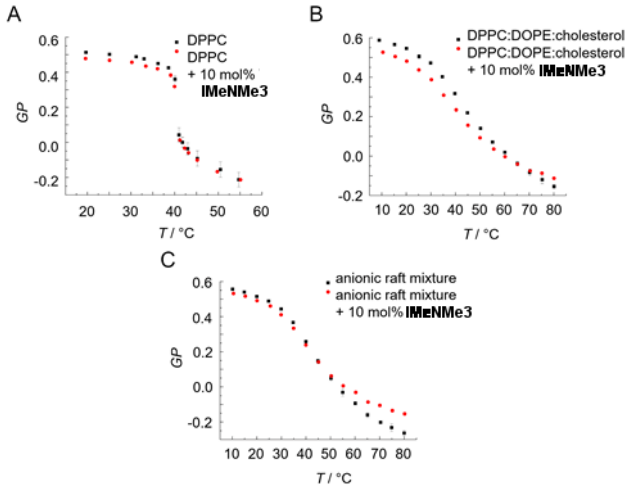

Figure 1. Representative results of the Laurdan *GP*-data for A) 1-, B) 3- and C) 5-component model biomembranes as a function of temperature. Black: without, red: with 10 mol% **IMeNMe$_3$**.

Fluorescence spectroscopy was used to gain insights into the impact of **IMeNMe$_3$** (10 mol%) on the lateral order and fluidity of the membrane. For this, the temperature-dependent behavior between 10 and 80 °C was analyzed using Laurdan[16] as a fluorescent probe. This fluorophore shows environment-dependent emission with a pronounced red-shift when changing from unpolar to more polar environments. The generalized polarization (*GP*) was recorded, with high values indicating a highly unpolar environment of Laurdan, which is found in laterally ordered gel phases. In contrast, the fluid phases show significant disorder within the lipid chains, allowing water molecules to diffuse into the upper chain region of the bilayer, causing a more polar environment and decreased *GP*-values (see SI for more details).

All *GP*-curves of the model membranes – both with and without **IMeNMe$_3$** – show a sigmoidal-like progression with increasing temperature. For the neat one-component bilayer, the main transition temperature was found at 41 °C with a decrease of the *GP*-values from 0.5 to values below zero during the gel-to-fluid phase transition, which is in good agreement with previous reports.[17] Upon addition of **IMeNMe$_3$** the main transition temperature is hardly affected, but slightly lower *GP*-values can be detected in the lipid-ordered region – indicating a marginally lower lipid packing density of the bilayer.

The same trend can be observed in the 3- (DPPC:DOPE:cholesterol) and 5-component lipid mixtures. Both lipid mixtures show a broader transition behavior in comparison to the 1-component model biomembrane, owing to the broad coexistence of liquid-ordered (l_o) and liquid-disordered (l_d) domains. An increase in temperature leads to an increasing amount of l_d domains, which is accompanied by an increase of fluidity and conformational disorder. The addition of 10 mol% **IMeNMe$_3$** results in a minor increase of the order parameter in the l_d phase (i.e. higher *GP*-values). This effect is more pronounced for the 5-component mixture than for the 3-component mixture. This observation might be associated with the attractive interaction between the cationic imidazolium and the anionic lipid headgroups.

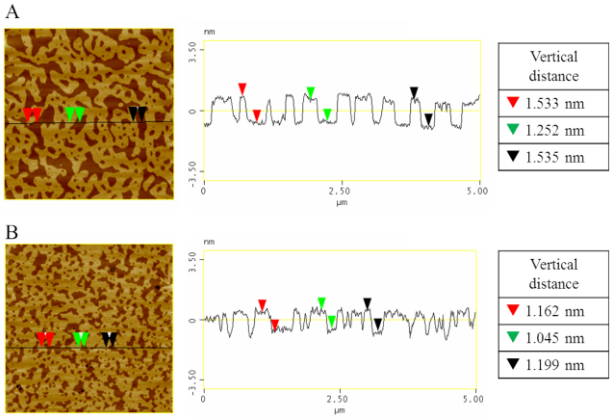

Figure 2. Characteristic AFM height images and cross-sectional area plots of the fully hydrated, 5-component model biomembrane A) without, B) with 10 mol% **IMeNMe$_3$**. The scan size of the images is 5 µm x 5 µm.

Additionally, atomic force microscopy (AFM) was used to detect possible **IMeNMe$_3$**-induced changes in lateral organization and membrane morphology by comparing domain heights and their distribution. To avoid membrane distortion, all measurements were executed in a fluid AFM cell in tapping mode, gaining information of the membrane structure in the fully hydrated state. The AFM height images of the 5-component lipid mixture with and without 10 mol% **IMeNMe$_3$** are shown in Figure 2. For the neat, 5-component lipid mixture, a height difference of 1.5 nm between l_o and l_d domains is detected, which is in good agreement with literature reports.[18] The addition of 10 mol% **IMeNMe$_3$** leads to slightly smaller l_d domains, while a minor decrease of the domain height difference to 1.1 nm is observed. These measurements show that **IMeNMe$_3$** readily inserts into the membrane but does not lead to drastic changes in the phase behavior or a disintegration of the lateral organization of the lipid bilayer.

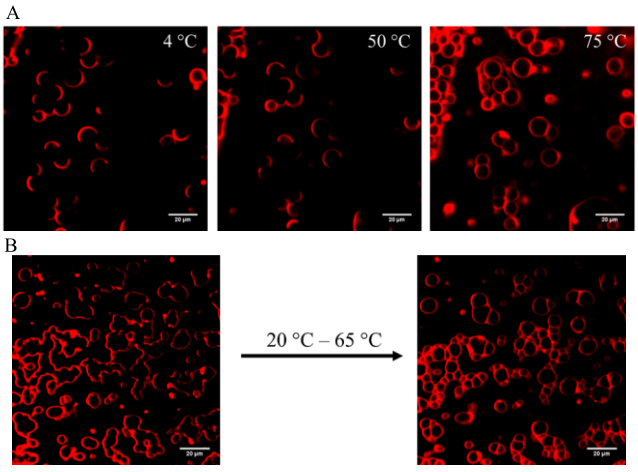

Figure 3. Representative confocal fluorescence microscopy cross-sectional images of GUVs with 10 mol% **IMeNMe$_3$** in A) the neutral 3-component model biomembrane at different temperatures and B) the anionic 5-component lipid vesicles with increasing temperature. GUVs labeled by *N*-rhodamine-DHPE. The scale bar represents 20 µm.

Furthermore, confocal fluorescence microscopy measurements were performed using giant unilamellar vesicles (GUVs). The lateral domain structure and the morphology of lipid vesicles were investigated upon addition of 10 mol% of **IMeNMe$_3$** to the neutral 3- (DPPC:DOPC:cholesterol) and the anionic 5-component model biomembrane. *N*-rhodamine-DHPE[16] was used as a fluorophore, which accumulates in the l_d domains of the GUVs.

For the 3-component model biomembrane, phase coexistence can be observed up to 50 °C. At 75 °C, an all-fluid phase can be detected (for images of the neat 3-component model membrane, see the SI). Interestingly, incorporation of **IMeNMe$_3$** induces an aggregation of the lipid vesicles. This effect is even more pronounced in the anionic 5-component model membrane, presumably due to stronger electrostatic interactions with the dicationic head group (Figure 3). For the 5-component model biomembrane, phase separation occurs at temperatures below 20 °C, which is seen on the interacting surfaces of the adherent vesicles, only. At around 65 °C an all-fluid phase is detected (images of the neat 5-component membrane can be found in the SI). The pronounced adherence of the lipid vesicles – most likely resulting from lipid sorting and interaction of the dicationic imidazolium salt with the negatively charged lipids DOPG and DPPG – suggests that **IMeNMe$_3$** could possibly induce membrane fusion, thus serving as a first verification of the feasibility of our initial compound design.

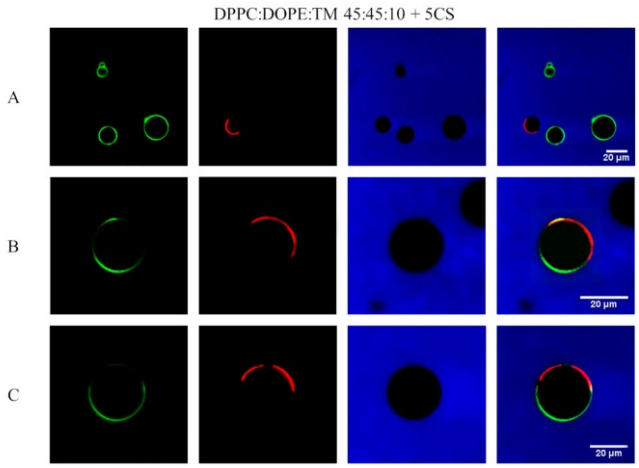

Figure 4. Confocal fluorescence microscopy cross-sectional images of the **IMeNMe$_3$** vesicle fusion experiments. First column: GUVs labeled by NBD-DHPE, Second column: GUVs labeled by *N*-rhodamine-DHPE; Third column: Buffer marked with Atto-647; Fourth column: Combined image. A) GUVs without **IMeNMe$_3$**, green – solid supported; target, red – added in bulk. B) GUVs with **IMeNMe$_3$**, green – solid supported; target, red – added in bulk. C) GUVs with **IMeNMe$_3$**, green – added in bulk; target, red – added in bulk. The scale bar of the images corresponds to 20 µm.

With these results in hand, we sought to investigate the fusogenic properties of **IMeNMe$_3$** in comparison to **IMeH** in a fluorescence microscopy-based assay. Therefore, a cargo lipid mixture of DPPC:DOPE (1:1) containing 10 mol% **IMeNMe$_3$** and the fluorophore NBD-DHPE[16] (green fluorescence; marking the l_o phase) was used. Here, due to its application as so-called helper lipid, DOPE was added. Helper lipids support induction of transient and local non-lamellar phases in the lipoplex membrane and therefore enhance internalization. For DOPE, the small ethanolamine headgroup promotes negative membrane curvature and therefore supports membrane fusion.[4,5,19]

As a target, a GUV of the 5-component lipid mixture labeled with *N*-rhodamine-DHPE (red fluorescence; marking the l_d phase) was chosen. GUVs with **IMeNMe$_3$** were prepared *via* electroformation and immobilized. The target vesicles were prepared employing polyvinyl alcohol (PVA)-assisted swelling and added to the bulk solution contacting the immobilized GUVs. Additionally, Atto-647 dye was inserted into the surrounding buffer, to evaluate the quality of vesicle fusion and to identify potential pore formation or leakage. The result was analyzed after an incubation time of 3 hours (see SI for more details).

In the absence of **IMeNMe$_3$**, neither close contact between both vesicle types, nor mixing of the fluorophores could be observed (Figure 4A). In the presence of **IMeNMe$_3$**, however, fusion of the vesicles could be detected, resulting in the coexistence of the fluorophores in the same GUV (Figure 4B), with the fused vesicles still showing l_o and l_d phase separation at room temperature. Also, no Atto dye was detected inside the vesicles, indicating that the fusion happens without membrane leakage. The same results were obtained when the target vesicle was prepared *via* electroformation, while the other vesicle was prepared *via* PVA-assisted swelling and added to the bulk solution. Preparing both vesicles by PVA-assisted swelling and adding them to the bulk medium also led to vesicle fusion without leakage as well (see Figure 4C).

Following the same preparation procedures, the fusogenic properties of the monocationic **IMeH** were investigated (see SI for details). Again, the vesicle interaction led to mixing of the two membrane fluorophores, indicating that also this derivative is able to induce fusion of lipid vesicles. Altogether, these data clearly indicate fusogenic properties of both imidazolium-based lipids, and thus support the design concept of imidazolium salts as valuable transfection vehicles.

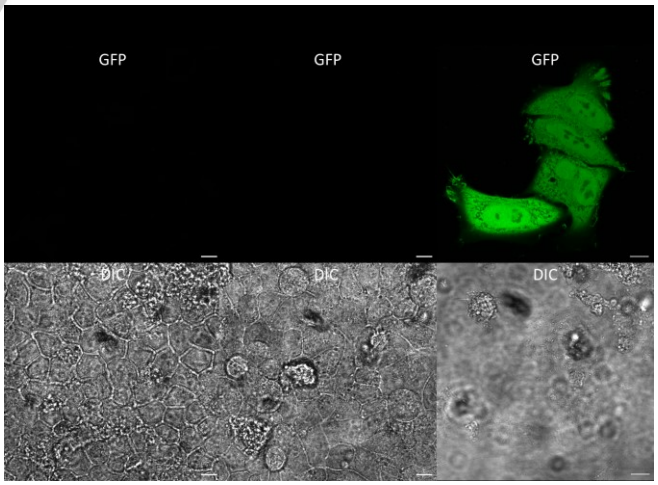

Figure 5. Liposome/**IMeNMe$_3$**-mediated transfection of a GFP plasmid into HeLa cells. A) No transfection reagent; B) Liposomes with **IMeH** as transfection reagent; C) Liposomes with **IMeNMe$_3$** as transfection reagent. Confocal microscopy images showing GFP fluorescence in the upper and phase contrast in the lower panels; scale bar 10 µm.

Given these detected fusogenic properties in the biophysical analyses, **IMeNMe$_3$** and **IMeH** were next employed in cellular studies. First, the cytotoxicity of the novel **IMeNMe$_3$** was evaluated by a lactate dehydrogenase assay, which confirmed that the molecule is tolerated by HeLa cells. Following, DPPC:DOPE (1:1) liposomes with an optimized loading of 20 mol% of the respective imidazolium salt, which were prepared *via* natural swelling, were incubated with cultured cells (HeLa) for 4 hours and the cells were then cultivated overnight (see SI for more details). To assess their potential for gene transfer, a green fluorescent protein (GFP) plasmid was added to the liposomes, which enabled the identification of successfully transfected cells through green fluorescence of the synthesized GFP.

As depicted in Figure 5, liposomes without imidazolium salt are unable to transfect the incorporated nucleic acid, i.e. no HeLa cells showing GFP fluorescence are identified. Similarly, cells treated with the **IMeH**-containing liposomes did not show expression of the GFP plasmid. However, when **IMeNMe$_3$**-containing liposomes were used, a successful transfection of the GFP plasmid was achieved resulting in the green fluorescence of the cells. Furthermore, the plasma membrane of the transfected cells remained intact as the cells failed to take up propidium iodide (see SI for more details).

This activity difference of the imidazolium salts justifies the design of **IMeNMe$_3$** and shows that the modification in the C2 position with a second positive charge is crucial for successful transfection. Most likely, the directional ammonium anchor protruding from the phospholipid bilayer could increase the strength of electrostatic interactions with nucleic acids and the negatively charged plasma membrane, thereby enabling transfection.

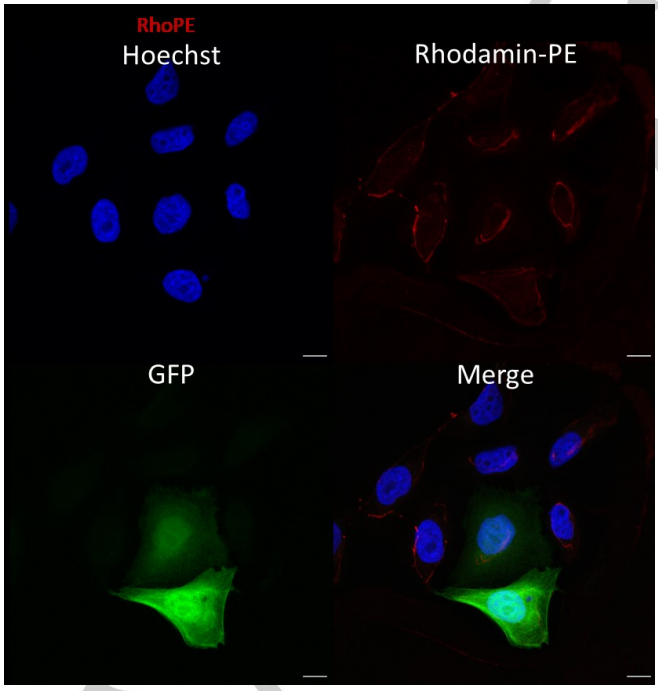

Figure 6. Transfection with **IMeNMe$_3$** liposomes containing Rhodamin-PE lipid to evaluate lipid distribution after transfection. Note that an enrichment of Rhodamin-PE in the plasma membrane can be observed. Blue – Hoechst, nuclear fluorescence. Red – Rhodamin-PE, lipid fluorophore. Green – expressed GFP; scale bar 10 µm.

To further study the transfection properties of **IMeNMe$_3$**, Rhodamine-PE (RhoPE, 1 mol%) was introduced as fluorescently labeled lipid into the liposome mixture and the cell interaction and fusion events were monitored over time. The data show that the liposomes appear to adhere to the cells prior to fusion and distribution of the rhodamine label in the plasma membrane (see SI for video). Furthermore, cells were fixed by paraformaldehyde (PFA) after incubation with the DPPC/DOPE/**IMeNMe$_3$**/RhoPE liposomes and GFP protein expression overnight. As depicted in Figure 6, an enrichment of RhoPE in the plasma membrane could again be observed, indicating successful membrane fusion. However, GFP plasmid expression could not be observed in every rhodamine-positive cell, suggesting a somewhat limited transfection efficiency, which was confirmed through quantitative analysis (see SI for further details)

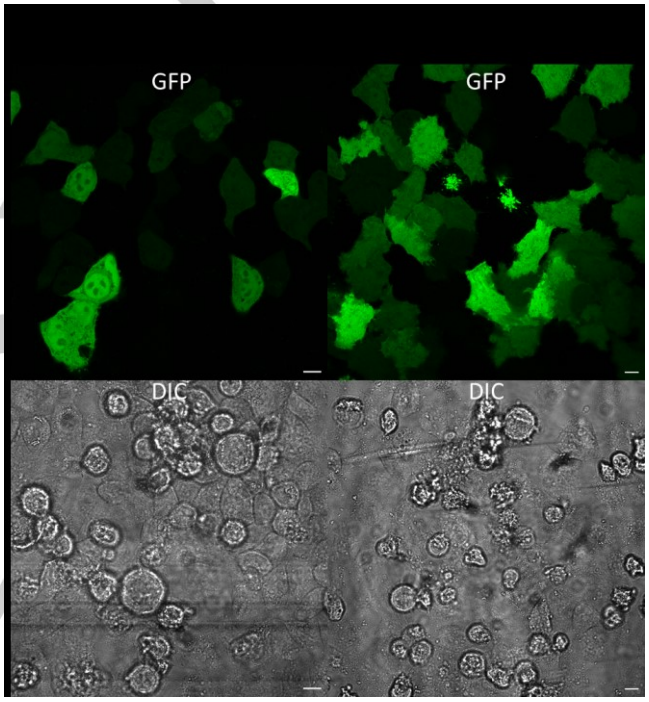

Figure 7. Comparison of IMeNMe3 and Lipofectamin2000™ as means for transfecting a GFP plasmid into HeLa cells. Cells were treated with IMeNMe3-containing liposomes or Lipofectamin2000™, incubated overnight and GFP expression was then monitored by confocal fluorescence microscopy; scale bar 10 µm.

This was further substantiated by comparing the transfection effectiveness of **IMeNMe$_3$** liposomal mixtures with that of the commercially available Lipofectamine 2000™ [20] as a well-established transfection agent, revealing lower transfection efficiency, but similar expression levels (as judged by fluorescence intensity) of the GFP protein (see Figure 7).

Beyond the previously discussed HeLa cells, we next evaluated the transfection effectiveness of **IMeNMe$_3$** in fibroblasts. As depicted in Figure 8, transfection of the GFP plasmid could be carried out successfully, albeit with lower efficiency than using Lipofectamin 2000.[20]

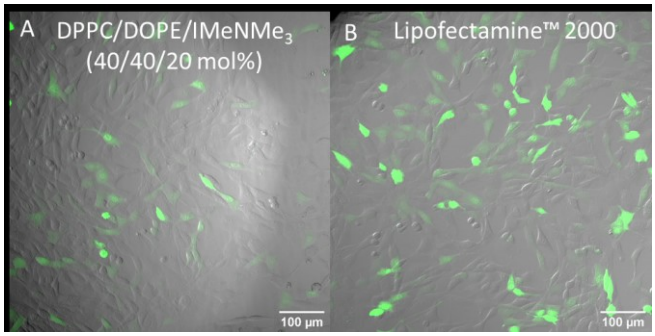

Figure 8: Representative confocal fluorescence microscopy images of IMeNMe3-liposomal transfection (DPPC/DOPE/IMeNMe3, A: 40/40/20 mol%, D:Lipofectamine™ 2000) of fibroblasts. Confocal microscopy images showing merge between GFP fluorescence and phase contrast; scale bar 100 µm.

Additionally, we investigated **IMeNMe$_3$** mediated transfection efficiency for another plasmid, which encoded the endosome targeting sequence Phe-Tyr-Val-Glu fused to GFP (2xFYVE-GFP). Figure SI 4 shows that HeLa cells were successfully transfected also with this plasmid, further expanding the scope of the reported transfection protocol.

With this proof-of-concept in hand, structural optimizations for further enhancement of lipofection efficiency of imidazolium salts are promising and ongoing in our laboratories. The observed reduced transfection efficiencies (as compared to Lipofectamin) could be attributed e.g. to low internalization rates or a hindered liberation of genetic material by the lipoplex. Both aspects could potentially be addressed through reagent design, exploiting the highly flexible synthetic route: Installing a bulkier ammonium anchor, or modifying the steric demand of the substituents at the head group are likely to affect its membrane integration and fusogenic behavior, whereas backbone substitution can be modified to support the induction of non-lamellar structures.

Conclusion

In conclusion, we have designed and tested the dicationic imidazolium salt **IMeNMe$_3$**, which readily integrates into different model biomembranes, leading to no deterioration of the lateral lipid organization or membrane disruption. Formation of a lipoplex using **IMeNMe$_3$** as an additive led to vesicle aggregation and induced membrane fusion with negatively charged vesicles. Based on this fusogenic potential, transfection protocols were designed and successful lipofection of a GFP or 2xFYVE plasmid into HeLa cells or fibroblasts was observed. In our lipid analogue concept, the alkyl ammonium moiety in the C2 position of the imidazolium enables electrostatic interactions with both the genetic material, and the target membrane. Thus, we provide a novel design for transfection agents, which are easily prepared and offer facile structural diversity. We believe that this structural motif will not only represent a platform for tailor-made transfection agents, thereby expanding the toolbox of lipoplex-mediated gene transfection, but also offer an easily modifiable reagent for the fundamental investigation of membrane fusion processes. Thus, we provide a novel design for transfection agents, which are easily prepared and offer facile access to structural diversity – addressing current challenges such as low efficiency across many cell types, and difficulties in cationic lipid preparation.

Acknowledgements

We thank Johannes Nass and Nikita Raj for providing the plasmids, as well as Tristan Wegner, Felix Strieth-Kalthoff and Toryn Dalton for helpful discussions. Financial support by the Deutsche Forschungsgemeinschaft (GRK 2515/1; SFB 858, EXC 1003 Cells in Motion Cluster of Excellence) is gratefully acknowledged. RW acknowledges funding from the Deutsche Forschungsgemeinschaft (DFG, German Research Foundation) under Germany's Excellence Strategy – EXC-2033 – Projektnummer 390677874.

Keywords: transfection • imidazolium • biophysics • liposomes • lipids

[1] a) T. K. Kim, J. H. Eberwine, *Anal. Bioanal. Chem.* **2010**, *397*, 3173–3178; b) L. Kaestner, A. Scholz, P. Lipp, *Bioorg. Med. Chem. Lett.* **2015**, *25*, 1171–1176; c) M. P. Stewart, R. Langer, K. F. Jensen, *Chem. Rev.* **2018**, *118*, 7409–7531.

[2] a) K. K. Hunt, S. A. Vorburger, *Science* **2002**, *297*, 415–416; b) M. L. Edelstein, M. R. Abedi, J. Wixon, R. M. Edelstein, *J. Gene Med.* **2004**, *6*, 597–602.

[3] a) D. Ferber, *Science* **2001**, *294*, 1638–1642; b) S. Hacein-Bey-Abina, C. von Kalle, M. Schmidt, F. Le Deist, N. Wulffraat, E. McIntyre, I. Radford, J. L. Villeval, C. C. Fraser, M. Cavazzana-Calvo, A. Fischer, *N. Engl. J. Med.* **2003**, *348*, 255–256; c) N. B. Woods, V. Bottero, M. Schmidt, C. von Kalle, I. M. Verma, *Nature* **2006**, *440*, 1123.

[4] a) P. L. Felgner, T. R. Gadek, M. Holm, R. Roman, H. W. Chan, M. Wenz, J. P. Northrop, G. M. Ringold, M. Danielsen, *Proc. Natl. Acad. Sci. USA* **1987**, *84*, 7413–7417; b) B. Ruozi, F. Forni, R. Battini, M. A. Vandelli, *J. Drug Target.* **2003**, *11*, 407–414; c) L. Wasungu, D. Hoekstra, *J. Control. Release* **2006**, *116*, 255–264; d) M. A. Mintzer, E. E. Simanek, *Chem. Rev.* **2009**, *109*, 259–302; e) H. Yin, R. L. Kanasty, A. A. Eltoukhy, A. J. Vegas, J. R. Dorkin, D. G. Anderson, *Nat. Rev. Genet.* **2014**, *15*, 541–555; f) fJ. Buck, P. Grossen, P. R. Cullis, J. Huwyler, D. Witzigmann, *ACS Nano* **2019**, *13*, 3754–3782.

[5] a) J. O. Rädler, I. Koltover, T. Salditt, C. R. Safinya, *Science* **1997**, *275*, 810–814; b) N. Dan, *Biochim. Biophys. Acta* **1998**, *1369*, 34–38; c) R. Koynova, B. Tenchov, R. C. Macdonald, *ACS Biomater. Sci. Eng.* **2015**, *1*, 130–138; d) C. Janich, A. Hädicke, U. Bakowsky, G. Brezesinski, C. Wölk, *Langmuir*, **2017**, *33*, 10172–10183.

[6] a) Y. Xu, F. C. Szoka, *Biochemistry* **1996**, *35*, 5616–5623; b) A. Coonrod, F. Q. Li, M. Horwitz, *Gene Ther.* **1997**, *4*, 1313–1321; c) H. H. Wang, A. Tsourkas, *Proc. Natl. Acad. Sci. USA* **2019**, *116*, 22132–22139.

[7] a) M. A. Kostiainen, J. G. Hardy, D. K. Schmith, *Angew. Chem. Int. Ed.* **2005**, *44*, 2556–2559; *Angew. Chem.* **2005**, *117*, 2612–2615; b) M. Rajesh, J. Sen, M. Srujan, K. Mukherjee, B. Sreedhar, A. Chaudhuri, *J. Am. Chem. Soc.* **2007**, *129*, 11408–11420; c) S. Bhattacharya, A. Bajaj, *Chem. Commun.* **2009**, 4632–4656; d) D. Zhi, S. Zhang, S. Cui, Y. Zhao, Y. Wang, D. Zhao, *Bioconjug. Chem.* **2013**, *24*, 487–519; e) N. A. Alhakamy, I. Elandaloussi, S. Ghazvini, C. J. Berkland, P. Dhar, *Langmuir*, **2015**, *31*, 4232-4245; f) A. Jarzebinska, T. Pasewald, J. Lambrecht, O. Mykhaylyk, L. Kümmerling, P. Beck, G. Hasenpusch, C. Rudolph, C. Plank, C. Dohmen, *Angew. Chem. Int. Ed.* **2016**, *55*, 9591–9595; *Angew. Chem.* **2016**, *128*, 9743–9747; g) L. Kudsiova, A. Mohammadi, M. F. M. Mustapa, F. Campbell, K. Welser, D. Vlaho, H. Story, D. J. Barlow, A. B. Tabor, H. C. Hailes, M. J. Lawrence, *Biomater. Sci.*, **2019**, *7*, 149–158; h) C. Van Bruggen, J. K. Hexum, Z. Tan, R. J. Dalal, T. M. Reineke, *Acc. Chem. Res.* **2019**, *52*, 1347–1358; i) R. Kanto,

Y. Qiao, K. Masuko, H. Furusawa, S. Yano, K. Nakabayashi, H. Mori, *Langmuir*, **2019**, *35*, 4646–4659; j) S. Dey, A. Gupta, A. Saha, S. Pal, S. Kumar, D. Manna, *ACS Omega*, **2020**, *5*, 735–750; k) M. R. Molla, S. Chakraborty, L. Munoz-Sagredo, M. Drechsler, V. Orian-Rousseau, P. A. Levkin, *Bioconjugate Chem.* **2020**, *31*, 852–860.

[8] Abbreviations for phospholipids: 1,2-dioleoyl-sn-glycero-3-phosphocholine (DOPC), 1,2-dipalmitoyl-sn-glycero-3-phosphocholine (DPPC), 1,2-dioleoyl-sn-glycero-3-phospho-(1'-rac-glycerol) sodium salt (DOPG), 1,2-dipalmitoyl-sn-glycero-3-phospho-(1'-rac-glycerol) sodium salt (DPPG), 1,2-dioleoyl-sn-glycero-3-phosphoethanolamine (DOPE).

[9] For an overview, see: M. N. Hopkinson, C. Richter, M. Schedler, F. Glorius, *Nature* **2014**, *510*, 485–496.

[10] L. Rakers, F. Glorius, *Biophys. Rev.* **2018**, *10*, 747–750.

[11] a) S. N. Riduan, Y. Zhang, *Chem. Soc. Rev.* **2013**, *42*, 9055–9070; b) C. M. Mahalakshmi, M. Karthick, M. Shanmugam, V. Chidambaranathan, *Sch. Res. Libr. Der Pharma Chem.* **2015**, *7*, 14–19; c) J. Gravel, A. R. Schmitzer, *Org. Biomol. Chem.* **2017**, *15*, 1051–1071.

[12] a) A. Rühling, H. J. Galla, F. Glorius *Chem Eur. J.* **2015**, *21*, 12291; b) D. Wang, C. Richter, A. Rühling, P. Drücker, D. Siegmund, N. Metzler-Nolte, F. Glorius, H. J. Galla, *Chem. - A Eur. J.* **2015**, *21*, 15123–15126; c) D. Wang, D. H. De Jong, A. Rühling, V. Lesch, K. Shimizu, S. Wulff, A. Heuer, F. Glorius, H. J. Galla, *Langmuir* **2016**, *32*, 12579–12592; d) P. Drücker, A. Rühling, D. Grill, D. Wang, A. Draeger, V. Gerke, F. Glorius, H. J. Galla, *Langmuir* **2017**, *33*, 1333–1342; e) A. Rühling, D. Wang, J. B. Ernst, S. Wulff, R. Honeker, C. Richter, A. Gerry, H. J. Galla, F. Glorius *Chem Eur. J.* **2017**, *23*, 5920–5924; f). Wang, H. J. Galla, P. Drücker, *Biophys. Rev.* **2018**, *10*, 735–746; g) T. Ghaed-Sharaf, D. S. Yang, S. Baldelli, M. H. Ghatee, *Langmuir* **2019**, *35*, 2780–2791; h) S. Mitra, R. Das, A. Singh, M. K. Mukhopadhyay, G. Roy, S. K. Ghosh, *Langmuir*, **2020**, *36*, 328–339; i) M. L. Stromyer, M. R. Southerland, U. Satyal, R. K. Sikder, D. J. Weader, J. A. Baughman, W. J. Youngs, P. H. Abbosh, *Eur. J. Med. Chem.,* **2020**, *185*, 111832; j) S. Bornemann, M. Herzog, L. Roling, T. O. Paulisch, D. Brandis, S. Kriegler, H. J. Galla, F. Glorius, R. Winter, Phys. Chem. Chem. Phys, **2020** DOI: 10.1039/D0CP00801J.

[13] a) K. S. Egorova, E. G. Gordeev, V. P. Ananikov, *Chem. Rev.* **2017**, *117*, 7132–7189; b) A. Benedetto, *Biophys. Rev.* **2017**, *9*, 309–320; c) K. S. Egorova, V. P. Ananikov, *J. Mol. Liq.* **2018**, *272*, 271–300; d) A. Benedetto, P. Ballone, *Langmuir* **2018**, *34*, 9579–9597; e) K. S. Egorova, V. P. Ananikov, *Biophys. Rev.* **2018**, *10*, 881-900.

[14] a) C. Samori, D. Malferrari, P. Valbonesi, A. Montecavalli, F. Moretti, P. Galletti, G. Sartor, E. Tagliavini, E. Fabbri, A. Pasteris, *Ecotoxicol. Environ. Saf.* **2010**, *73*, 1456–1464; b) E. B. Anderson, T. E. Long, *Polymer* **2010**, *51*, 2447–2454; c) K. Rawat, H. B. Bohidar, *J. Phys. Chem. B* **2012**, *116*, 11065–11074; d) M. Tischer, G. Pradel, K. Ohlsen, U. Holzgrabe, *ChemMedChem* **2012**, *7*, 22–31.

[15] a) J. Pernak, K. Sobaszkiewicz, I. Mirska, *Green Chem.* **2003**, *5*, 52–56; b) D. Demberelnyamba, K. S. Kim, S. Choi, S. Y. Park, H. Lee, C. J. Kim, I. D. Yoo, *Bioorganic Med. Chem.* **2004**, *12*, 853–857; c) L. Carson, P. K. W. Chau, M. J. Earle, M. A. Gilea, B. F. Gilmore, S. P. Gorman, M. T. McCann, K. R. Seddon, *Green Chem.* **2009**, *11*, 492–497; d) A. Cornellas, L. Perez, F. Comelles, I. Ribosa, A. Manresa, M. T. Garcia, *J. Colloid Interface Sci.* **2011**, *355*, 164–171.

[16] Abbreviations for fluorophores: *N*-(7-nitrobenz-2-oxa-1,3-diazol-4-yl)-1,2-dihexadecanoyl-sn-glycero-3-phosphoethanolamine (NBD-DHPE); *N*-(LissamineTM Rhodamin B sulfonyl)-1,2-dihexadecanoyl-sn-glycero-3-phosphoethanol-amine (N-rhodamine-DHPE); 6-dodecanoyl-*N,N*-dimethyl-2-naphthylamine (Laurdan).

[17] R. Winter, F. Noll, C. Czeslik, *Methoden Der Biophysikalischen Chemie*, Vieweg + Teubner, Wiesbaden, **2011**.

[18] a) H. A. Rinia, M. M. E. Snel, J. P. J. M. van der Eerden, B. de Kruijff, *FEBS Lett.* **2001**, *501*, 92–96; b) K. Weise, G. Triola, L. Brunsveld, H. Waldmann, R. Winter, *J. Am. Chem. Soc.* **2009**, *131*, 1557–1564; c) M. Dwivedi, T. Mejuch, H. Waldmann, R. Winter, *Angew. Chem. Int. Ed.* **2017**, *56*, 10511–10515; *Angew. Chem.* **2017**, *129*, 10647-10651.

[19] a) D. C. Litzinger, L. Huang, *Biochim. Biophys. Acta* **1992**, *1113*, 201–227; b) H. Farhood, N. Serbina, L. Huang, *Biochim. Biophys. Acta* **1995**, *1235*, 289–295; c) S. D. Patil, D. G. Rhodes, D. J. Burgess, *AAPS J.* **2004**, *6*, 13–22.

[20] a) B. Dalby, S. Cates, A. Harris, E. C. Ohki, M. L. Tilkins, P. J. Price, V. C. Ciccarone, *Methods* **2004**, *33*, 95–103; b) J. J. Green, R. Langer, D. G. Anderson, *Acc. Chem. Res.* **2008**, *41*, 749–759; c) Y. C. Tseng, S. Mozumdar, L. Huang, *Adv. Drug Deliv. Rev.* **2009**, *61*, 721–731; d) F. Cardarelli, L. Digiacomo, C. Marchini, A. Amici, F. Salomone, G. Fiume, A. Rossetta, E. Gratton, D. Pozzi, G. Caracciolo, *Sci. Rep.* **2016**, *6*, 25879.

10.1002/chem.202003466

Entry for the Table of Contents

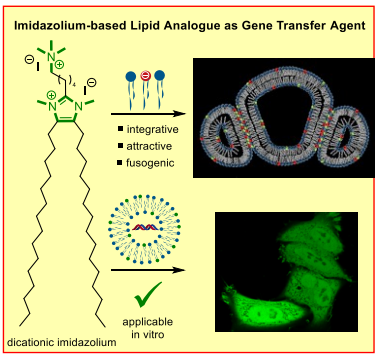

Can't get transfection? A transfection reagent based on a dicationic imidazolium salt was developed. Detailed analyses of membrane incorporation, adhesion of vesicles and fusogenic properties of the salt are described. Cell experiments show the successful *in vivo* application of this new class of transfection reagents.